University of Groningen

Splicing factor TRA2A contributes to esophageal cancer progression via a noncanonical role in lncRNA m⁶A methylation

Bei, Mingrong; Hao, Shijia; Lin, Kai; Chen, Qiuyang; Cai, Yujie; Zhao, Xing; Jiang, Leiming; Lin, Lirui; Dong, Geng; Xu, Jianzhen

IMPORTANT NOTE: You are advised to consult the publisher's version (publisher's PDF) if you wish to cite from it. Please check the document version below.

Document Version
Publisher's PDF, also known as Version of record

Publication date:
2023

Link to publication in University of Groningen/UMCG research database

ORIGINAL ARTICLE

Splicing factor TRA2A contributes to esophageal cancer progression via a noncanonical role in lncRNA m[6]A methylation

Mingrong Bei[1] | **Shijia Hao[1]** | **Kai Lin[2,3]** | **Qiuyang Chen[1]** | **Yujie Cai[4]** | **Xing Zhao[1,5]** | **Leiming Jiang[1]** | **Lirui Lin[1,3]** | **Geng Dong[2,3]** | **Jianzhen Xu[1,3]** (ORCID)

[1]Systems Biology Laboratory, Shantou University Medical College (SUMC), Shantou, China

[2]Department of Biochemistry and Molecular Biology, Shantou University Medical College (SUMC), Shantou, China

[3]Guangdong Provincial Key Laboratory of Infectious Diseases and Molecular Immunopathology, Shantou University Medical College, Shantou, China

[4]Guangdong Key Laboratory of Age-Related Cardiac and Cerebral Diseases, Affiliated Hospital of Guangdong Medical University, Zhanjiang, China

[5]Department of Pathology and Medical Biology, University of Groningen, University Medical Center, Groningen, The Netherlands

Correspondence
Jianzhen Xu, Systems Biology Laboratory, Shantou University Medical College (SUMC), 22 Xinling Road, Shantou 515041, China.
Email: jzxu01@stu.edu.cn

Funding information
Guangdong Provincial Key Laboratory of Infectious Diseases and Molecular Immunopathology

Abstract

Transformer 2 alpha homolog (TRA2A), a member of the serine/arginine-rich splicing factor family, has been shown to control mRNA splicing in development and cancers. However, it remains unclear whether TRA2A is involved in lncRNA regulation. In the present study, we found that TRA2A was upregulated and correlated with poor prognosis in esophageal cancer. Downregulation of TRA2A suppressed the tumor growth in xenograft nude mice. Epitranscriptomic microarray showed that depletion of TRA2A affected global lncRNA methylation similarly to the key m[6]A methyltransferase, METTL3, by silencing. MeRIP-qPCR, RNA pull-down, CLIP analyses, and stability assays indicated that ablation of TRA2A reduced m[6]A-modification of the oncogenic lncRNA MALAT1, thus inducing structural alterations and reduced stability. Furthermore, Co-IP experiments showed TRA2A directly interacted with METTL3 and RBMX, which also affected the writer KIAA1429 expression. Knockdown of TRA2A inhibited cell proliferation in a manner restored by RBMX/KIAA1429 over-expression. Clinically, MALAT1, RBMX, and KIAA1429 were prognostic factors of worse survival in ESCA patients. Structural similarity-based virtual screening in FDA-approved drugs repurposed nebivolol, a β_1-adrenergic receptor antagonist, as a potent compound to suppress the proliferation of esophageal cancer cells. Cellular thermal shift and RIP assay indicated that nebivolol may compete with MALAT1 to bind TRA2A. In conclusion, our study revealed the noncanonical function of TRA2A, which coordinates with multiple methylation proteins to promote oncogenic MALAT1 during ESCA carcinogenesis.

KEYWORDS
esophageal cancer, LncRNA methylation, MALAT1, splicing factor, TRA2A

1 | INTRODUCTION

Esophageal cancer ranks seventh in incidence and sixth in mortality of all cancers, accounting for ~604,000 new cases and ~544,000 deaths in 2020 in 158 countries.[1] Although chemoradiotherapy, immunotherapy, and surgical treatment have advanced and been optimized, esophageal cancer still has a poor prognosis with a 5-year survival rate of only 12%–20%.[2] Esophageal cancer can be classified into two major subtypes, including ESCC and EAC.[3] Cigarette smoking and heavy drinking are the main risk factors for ESCC, while EAC is mainly associated with chronic gastroesophageal reflux disease (GERD), obesity, and cigarette smoking.[4,5] Recent studies have reported that chemotherapy (docetaxel or paclitaxel) plus nivolumab (a PD-1 inhibitor) offers a clinically meaningful overall survival benefit for esophageal cancer patients, but nivolumab may contribute to loss of peripheral tolerance and subsequently lead to autoimmunity.[2,6] Even though some patients have a high positive response to chemotherapy and immunotherapy in the early stage, most will still develop drug resistance over time due to unknown mechanisms.[6,7] Thus, it is important to understand the molecular mechanism of oncogenesis and progression.

The serine/arginine (SR)-rich protein family is a major class of splicing factors, and plays an instrumental role in mRNA splicing.[8] They harbor RRM that bind to specific RNA sequences, and arginine/serine-rich (RS) domains that coordinate with other proteins to function properly.[8] TRA2A is an abnormally overexpressed SR protein in esophageal cancers.[9,10] It was first found to control hermaphrodite development in *Caenorhabditis elegans*.[11] In cancers, TRA2A not only accelerates the progression of glioma,[12] but is also involved in promoting drug resistance and tumor progression in triple-negative breast cancer in an AS-dependent manner.[13]

Except for this canonical function, recent evidence has indicated that SR protein can also interact with lncRNAs to form a functional entity, thus driving oncogenesis and evading anticancer drug treatments.[14,15] Through analysis of CLIP data, we identified multiple oncogenic lncRNAs as TRA2A partners, such as KTN1–AS1, CCDC183–AS1, and MALAT1 (Table S1). In esophageal cancer cells, we confirmed TRA2A–MALAT1 binding using a complementary RNA pull-down assay and reported that this interaction triggered carcinogenesis via the EZH2/β-catenin axis.[9] The binding to multiple lncRNAs suggests that TRA2A may exert its regulatory role via a mechanism independent of its regulation of mRNA splicing. In this study, we engineered TRA2A-knockdown human esophageal cancer cells to investigate its detailed mechanism. We found that attenuation of TRA2A inhibited tumor growth in vivo. Downregulation of TRA2A caused global changes in lncRNA m⁶A-methylation. Especially, TRA2A may drive carcinogenesis via MALAT1 methylation in esophageal cancer.

2 | MATERIALS AND METHODS

2.1 | Cell culture and treatment

TE1, KYSE150 and the human embryonic kidney (HEK) cell line HEK293T were obtained from the Cell Resource Center of the Shanghai Institute of Life Science (China) and maintained according to standard protocols. For the generation of shTRA2A, shRNAs targeting TRA2A-specific regions and a negative control scrambled shRNA were cloned into the pLKO.1 vector. To overexpress RBMX and KIAA1429, the cDNAs encoding RBMX and KIAA1429 were inserted into the pCDNA3.1 vector followed by adding a Flag tag, and the empty vector acting as the negative control. siRNA oligonucleotides were synthesized by GenePharma Company (China; sequences are listed in Table S2). Transfection of plasmids and siRNAs was performed using Lipofectamine 3000 (Invitrogen). For the cytotoxic assay, nebivolol hydrochloride and other compounds were purchased from TopScience Company (China).

2.2 | Generation of TRA2A knockdown cell lines

pLKO.1 lentiviral vectors including control vector with lentivirus packaging mix were co-transfected into HEK293T cells to generate TRA2A shRNA-encoding lentivirus and control lentivirus. After 48 h of infection, cells were selected in a growth medium supplemented with puromycin (1.5 μg/mL for TE1 and 3 μg/mL for KYSE150) for 2 weeks, until a stably growing population arose.

2.3 | RNA extraction, cDNA synthesis and RT-PCR

Total RNA was extracted using TRIzol (Invitrogen). DNA removal and cDNA synthesis were performed using a PrimeScript RT reagent kit with gDNA Eraser (TaKaRa). RT-PCR was performed using the TB Green Premix Ex Taq II (TaKaRa) and the reactions were subsequently measured using an ABI QS5 Real Time PCR instrument (Thermo Fisher Scientific). The target gene was quantified using the $2^{-\Delta\Delta C_t}$ method. Primer sequences are listed in Table S2.

2.4 | Epitranscriptomic microarray, MeRIP-qPCR and RIP-qPCR

Total RNA was isolated from TE1 TRA2A-knockdown and control cells. RNA quantification and integrity were assessed using a NanoDrop ND-1000 spectrophotometer and denaturing agarose gel electrophoresis, respectively. Sample preparation and microarray hybridization were performed according to Arraystar's protocols. For global lncRNA analysis, the m⁶A quantities of all lncRNAs were added together and a paired t-test was used for group

comparison. The epitranscriptomic microarray dataset is available at the National Genomics Data Center of China with accession number PRJCA009954 (https://ngdc.cncb.ac.cn/?lang=en). MeRIP assay was performed using the EpiQuik CUT&RUN m^6A RNA Enrichment Kit (EpigenTek). RIP was performed using the Magna Nuclear RIP Kit (Millipore). RNA fragments were eluted from magnetic beads and determined using One-step RT-PCR (Transgene Biotech). Specific primers are listed in Table S2.

2.5 | RNA pull-down assay

The MALAT1 sequence (NR_002819.3) was divided into four fragments of ~2 kbp and cloned into the pEASY-blunt vector that was transcribed by the T7 promoter in vitro. Labeled RNA was mixed with magnetic beads and then incubated with cell lysates to elute the protein–MALAT1 complex. Proteins associated with biotin-labeled RNAs were immunoprecipitated using streptavidin magnetic beads, and subjected to isobaric tags for relative and absolute quantitation (iTRAQ) experiments using an AB SCIEX TripleTOF® 6600 System and AB SCIEX ProteinPilot™ 4.5 software.

2.6 | RNA stability assay

Cells were seeded into dishes to adhere overnight. After treatment with actinomycin D (10 μg/mL, Selleck), total RNA was harvested at 0, 3, and 6 h using TRIzol or following the luciferase reporter assay. The RNA degradation rate was estimated by comparison with 0 h.

2.7 | Luciferase reporter assay

The wild-type and mutant TRA2A-binding-motif sequences of MALAT1 were synthesized and inserted into the psicheck2-basic firefly/renilla luciferase vector. Cells were seeded into a 24-well plate followed by co-transfection with reporter plasmid and the TRA2A siRNA or TRA2A overexpression plasmid. After 24–48 h, cells were harvested to access luciferase activity using the Dual-Lumi Reporter Kit (Beyotime). Relative luciferase activity was assessed by the ratio of renilla and firefly luciferase values.

2.8 | Western blotting and Co-IP

Cells were lysed in RIPA buffer with 1 mM PMSF (Solarbio), then centrifuged at 4°C and 12,000 rpm to pellet the debris. The supernatants were boiled in SDS sample buffer, resolved on 10% SDS-PAGE gels and transferred onto 0.22-μm PVDF membranes (Millipore). Co-IP was performed according to the manufacturer's procedure (Absin). The following antibodies were used: rabbit anti-TRA2A (1:1000, 72625, Abcam), rabbit anti-GADPH (1:1000, 2118, CST), rabbit anti-RBMX (1:1000, 14794, CST), rabbit anti-KIAA1429

(1:1000, 88358, CST), rabbit anti-Flag (1:2000, 20543, Proteintech), mouse anti-Flag (1:2000, 66008, Proteintech), rabbit anti-EZH2 (1:4000, 5246, CST), rabbit anti-β-catenin (1:1000, 8480, CST), anti-rabbit IgG-HRP (1:1000, 7074, CST), and anti-mouse IgG-HRP (1:2000, 7076, CST).

2.9 | Cell proliferation assay and colony formation assay

Proliferation was measured using the Cell Counting Kit-8 (Boster). For colony formation, 400 cells were seeded into six-well plates per well. After incubation for 12 days, 4% paraformaldehyde (Solarbio) was used to fix the cells, then 0.1% crystal violet solution (Beyotime) was used to stain the colonies.

2.10 | Animal experiments

Four-week-old male nude mice used for tumor growth studies were purchased from GemPharmatech Company (China) and divided randomly into two groups. Scramble and TRA2A knockdown KYSE150 cells (4.74×10^6 cells in 100 μL Matrigel, Corning) were injected subcutaneously into the left flanks of the mice. The tumor sizes were measured 1 week after injection and tumor volumes were estimated every 3 or 4 days (volume = length × width^2 × 0.5). Upon termination of the experiment, mice were euthanized and their tumors were removed.

2.11 | Bioinformatics analysis

RNA-seq data after deletion of TRA2A using CRISPR were downloaded from ENCODE (https://www.encodeproject.org/). m^6A sites were predicted using SRAMP (http://www.cuilab.cn/sramp). Using the 'cugaaga' motif from the RBPmap (http://rbpmap.technion.ac.il/), we predicted the potential binding sites along the MALAT1 sequence. CLIP-seq data for TRA2A were downloaded from ENCODE and annotated using ChIPseeker.[16] The lncRNA annotations were obtained from LNCipedia (https://lncipedia.org/). The m^6A-seq data for shTRA2A in HepG2 cells were accessed from the SRA with ID PRJNA551046 (https://www.ncbi.nlm.nih.gov/sra). RNA2DMut analysis of potential mutated nucleic acid was conducted at the RNA2DMut website (https://rna2dmut.bb.iastate.edu). The m^6A-seq data for shMETTL3 in KYSE-30 cells were accessed with ID SRP309472 from the SRA. DESeq2 (http://www.bioconductor.org/packages/release/bioc/html/DESeq2.html) was used for differential analysis. Because of the different annotations between the epitranscriptomic microarray and sequencing data, we downloaded lncRNA symbols from Ensembl (11964 lncRNAs in total) to re-annotate the shTRA2A-MeRIP data. Cancer-related lncRNAs were obtained from LncRNADisease,[17] enrichment analysis was performed using the chi-squared test.

2.12 | Virtual screening

A molecular similarity-based method was used for screening. Indacaterol was used as a reference to select a candidate inhibitor from the FDA-approved drugs using ChemMapper.[18] Top 400 molecules that had similarities to the three-dimensional shape and surface electrostatic properties were selected. Molecular docking was performed using the Autodock Vina program,[19] similar to that described in our previous study.[20] TRA2A structure was obtained from alphafold2. The binding site was set to the RRM domain with residue numbers 119–197. The docking box was set as a cube of $10\text{Å}\times10\text{Å}\times10\text{Å}$ centered at $(-5.4, -1.1, -6.9)$.

2.13 | Cellular thermal shift assay

Cells were pre-treated with $50\,\mu\text{M}$ nebivolol hydrochloride for 3h, then 6×10^5 cells were suspended in PBS containing $1\times$ Protease inhibitor cocktail (Beyotime). The cells were snap frozen in liquid nitrogen, then rapidly thawed at 37°C three times to break the cells. The cell lysates were centrifuged at $14,000\,g$ for 30min at 4°C to pellet the cellular debris and the supernatant was heated in a temperature gradient followed by western blot.

2.14 | Statistical analysis

Statistical analyses were performed using SPSS (IBM) and GraphPad Prism 8.0 software. All data were collected from at least three independent experiments and data were presented as the mean $\pm$ standard error of the mean (SEM) using a t-test or one-way analysis of variance test. p-values <0.05 were considered to indicate significance.

3 | RESULTS

3.1 | TRA2A is an oncogenic gene and is correlated with ESCA prognosis

We have previously shown that silencing of TRA2A inhibits proliferation, colony formation, and migration of esophageal cancer cells.[9] To study the function of TRA2A in vivo, we engineered TRA2A-knockdown TE1 and KYSE150 cell lines by infecting cells with lentivirus encoding TRA2A shRNA. The reduced TRA2A expression in esophageal cells was verified using both RT-PCR and western blotting (Figure 1A,B). Through inoculation of TRA2A-knockdown and control KYSE150 cells subcutaneously into nude mice, we observed that knockdown of TRA2A resulted in decreased tumor volume and tumor weight (Figure 1C–E). We next confirmed the correlation between TRA2A and clinical parameters in the ESCA cohort of TCGA. The results showed that the TRA2A mRNA levels were upregulated in esophageal cancer patients compared with the normal patients

(Figure 1F). In addition, high expression of TRA2A correlated with low overall survival and disease-free survival in esophageal cancer patients (Figure 1G,H). Collectively, these results suggest that knockdown of TRA2A inhibits tumor growth in vivo and high expression of TRA2A correlates with poor prognosis in ESCA.

3.2 | TRA2A regulates global lncRNA methylation in esophageal cancer cells

Recently, An et al.[21] found that TRA2A directly interacts with METTL3, the major catalytic component of m6A methyltransferase, in liver cancer. To investigate the role of TRA2A in RNA methylation, we first compared the expression pattern in ESCA patient cohorts from TCGA, and found that METTL3 was correlated with TRA2A (Figure 2A). After TRA2A knockdown in TE1 and KYSE150 cells, METTL3 mRNA levels were accordingly decreased (Figure 2B). Co-IP assay indicated that TRA2A directly interacted with METTL3 in TE1 and KYSE150 cells (Figure 2C). Then, we performed a MeRIP microarray of TRA2A knockdown in TE1 esophageal cancer and control cells (Figure 2D). Notably, the total m6A level of lncRNAs decreased in the TRA2A-knockdown cells ($p=3.00\text{e-}02$), indicating that TRA2A may regulate global lncRNA methylation (Figure 2E). To further verify its role, we compared the methylation profiles either after the knockdown of TRA2A or depletion of METTL3. We found that the m6A profiles of 1713 lncRNAs were altered after the knockdown of METTL3, among which 37 lncRNAs were similarly altered after the knockdown of TRA2A (Figure 2F; chi-squared test, $p=1.90\text{e-}05$). The significant overlapping lncRNAs suggested that TRA2A is involved in the core methylation process and promoted similar modification on lncRNAs as does METTL3. Moreover, the TRA2A-dependent m6A methylation lncRNAs were significantly enriched with known cancer-associated lncRNAs (Figure 2G; chi-squared test, $p=2.93\text{e-}02$), which indicated that TRA2A might tightly regulate lncRNAs in esophageal cancer in an m6A-dependent manner.

3.3 | TRA2A modulates MALAT1 stability via m6A-dependent manner

We previously found that MALAT1, an oncogenic lncRNA, was regulated by TRA2A.[9] Genetic deletion of TRA2A via CRISPR also led to decreased MALAT1 expression ($p=5.00\text{e-}02$; Table S3). RNA pull-down assay suggested that TRA2A mainly bound to the region at 2341 - 4500nt (Table S4). Using a complementary analysis of the CLIP data after the shRNA knockdown of TRA2A also indicated potential binding sites in MALAT1 (Figure 3A). Furthermore, we used RBPmap to predict the TRA2A binding sites along the MALAT1 fragment according to the binding motif "cugaaga." Collectively, we concluded that the most likely TRA2A binding sites were at 2373–2391nt, 2465–2492nt, and 2828–2842nt on MALAT1 (Figure 3A). To further demonstrate the TRA2A binding
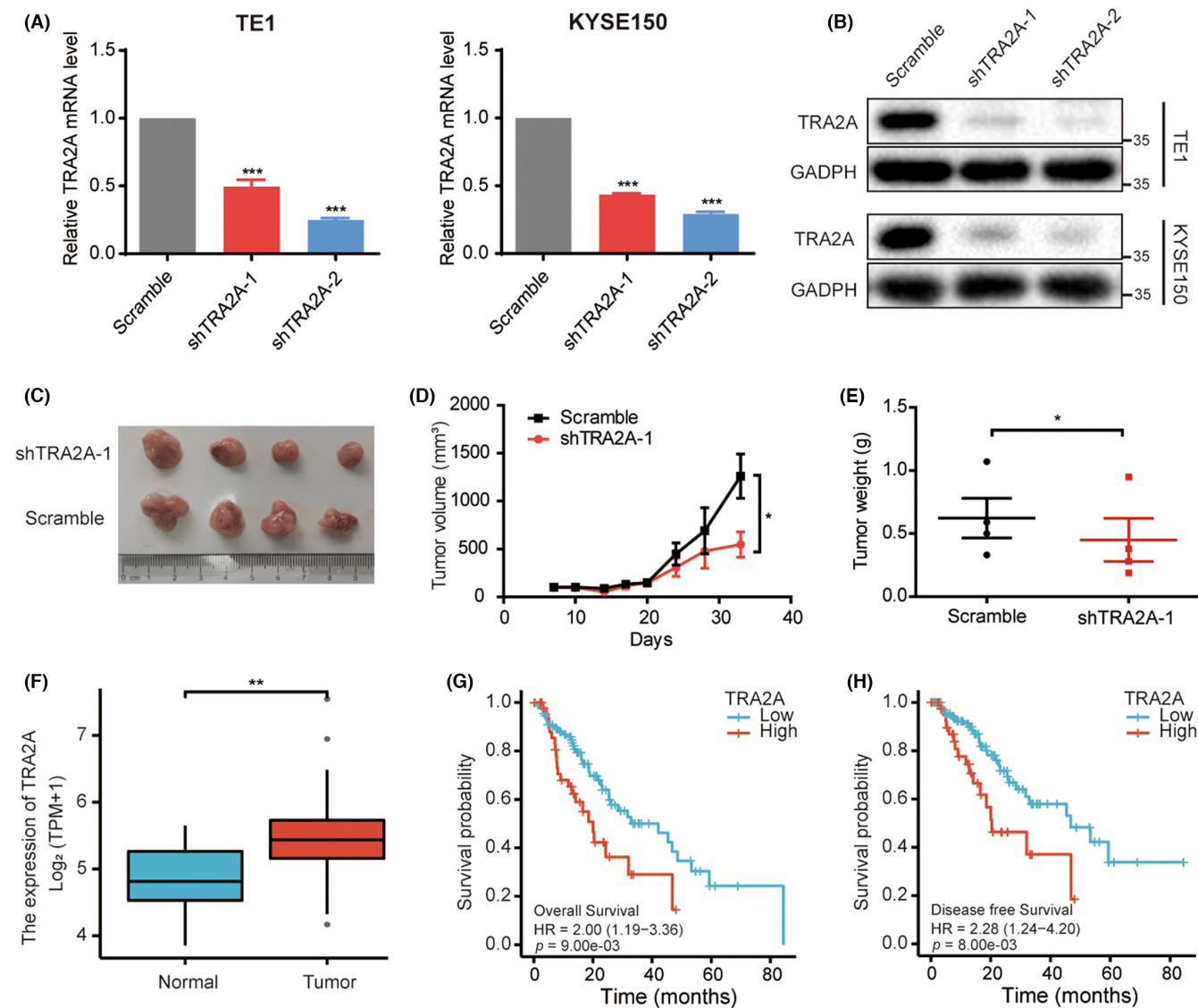
FIGURE 1 TRA2A is oncogenic in ESCA. (A, B) RT-PCR and western blot analysis of the mRNA and protein levels of TRA2A in TE1 and KYSE150 cells after infection with scramble or shTRA2A lentivirus, $n=3$. (C) Xenograft tumors formed by subcutaneously injecting KYSE150-scramble or KYSE150-shTRA2A cells into nude mice, $n=4$. (D, E) Tumor volume was compared at Day 33 and tumor weight was measured after the experiment. (F) mRNA expression in the ESCA cohort from TCGA, $n=173$. (G, H) Overall survival rate and disease-free survival rate of patients in TCGA, with a comparison between the low and high TRA2A expression groups, $n=173$. Data are expressed as mean $\pm$ SEM; $^*p<0.05$, $^{**}p<0.01$.

sites on MALAT1, we mutated the TRA2A binding motif (2828–2835 nt) of MALAT1 and inserted it into a dual-luciferase reporter vector (Figure 3B). As expected, the luciferase activity of the MALAT1-Mut plasmid was lower than that of the MALAT1-WT plasmid in 293T cells after transfection for 24 h (Figure 3C). Also, the half-life of luciferase of MALAT-1-Mut was shorter than that of MALAT1-WT in both TE1 and KYSE150 cells (Figure 3D). Furthermore, the luciferase activity of cells transfected with MALAT1-WT plasmids tended to decrease when TRA2A was silenced compared with the MALAT1-Mut group (Figure 3E) and analogous results could be verified in TRA2A-overexpression cells (Figure 3F). These results implied that the TRA2A binding motif is essential for the stability of MALAT1.

We aligned the m⁶A modification peaks in shTRA2A HepG2 cells on the MALAT1 sequence (Figure 3A). Interestingly, there were several m⁶A sites surrounding TRA2A binding sites on MALAT1. One enriched m⁶A peak was positioned at 2625–2700 nt. In addition, the m⁶A site at 2539–2744 nt was predicted with very high confidence using the SRAMP database (Figure 3G). Therefore, we hypothesized that TRA2A affects m⁶A methylation on MALAT1, at sites co-localized with TRA2A binding site. Taken together, the 2539–2744 nt fragment of MALAT1 mRNA was used to design primers for verification. A MeRIP-qPCR assay was performed to investigate the m⁶A status of MALAT1. Our results showed that the m⁶A marks in the MALAT1 sequence were enriched in esophageal cancer cells (Figure 3H), while downregulation of TRA2A caused a methylation

FIGURE 2 TRA2A regulates global lncRNA methylation. (A) Correlated expression between TRA2A and METTL3 in ESCA from TCGA ($n=197$). (B) mRNA levels of METTL3 after TRA2A knockdown in TE1 and KYSE150 cells ($n=3$). (C) Western blots showing the interaction between TRA2A and METTL3. (D) Heatmap of lncRNA m^6A quantity in scramble or shTRA2A TE1 cells, $n=3$. (E) Global m^6A levels were compared between scramble or TRA2A knockdown cells ($n=3$). (F) TRA2A-dependent lncRNAs significantly overlap with that of METTL3-dependent lncRNAs. (G) TRA2A-dependent lncRNAs are also known cancer-related lncRNAs. Data are expressed as mean±SEM; *$p<0.05$, **$p<0.01$, ***$p<0.001$.
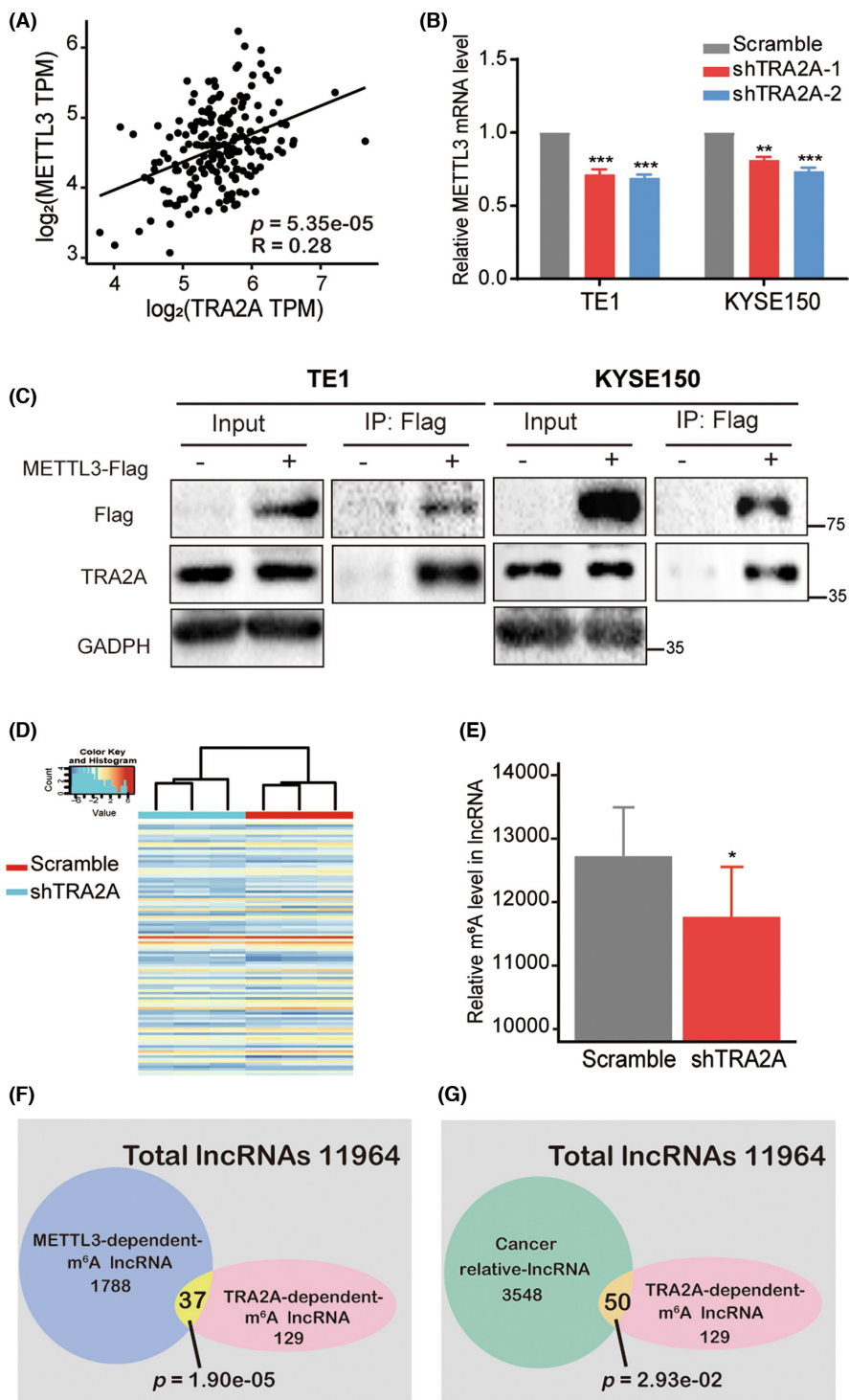

FIGURE 3 TRA2A regulates lncRNA MALAT1 methylation and stability. (A) TRA2A binding sites on MALAT1 by RBPmap analysis, CLIP and m^6A-seq datasets. (B) Graphical map for luciferase reporter construction. (C) Relative luciferase activity in 293T cells after transfection with MALAT1-WT or MALAT1-Mut plasmids, $n=3$. (D) Luciferase-MALAT1-WT and MALAT1-Mut decay rates were determined in TE1 and KYSE150 cells after treatment with actinomycin D, $n=3$. (E, F) Relative luciferase activity in TE1 and KYSE150 cells after co-transfection of siTRA2A or TRA2A overexpression plasmids with MALAT1-WT or MALAT1-Mut plasmids, $n=3$. (G) SRAMP prediction of the m^6A sites on MALAT1. (H) MeRIP-qPCR to determine N^6-modification on MALAL1, $n=3$. (I) MeRIP-qPCR was performed to identify variation in N^6-methylation level enrichment in MALAT1 after silencing of TRA2A, $n=3$. (J) Predicted structural changes and stability of MALAT1. Deep red highlights mutations contributing to an unstable MALAT1 structure. The larger 'A's indicate potential methylated adenine ribonucleotides. (K) MALAT1 decay rates were determined in TE1 and KYSE150 cells after treatment with actinomycin D, $n=3$. Data are expressed as mean±SEM; *$p<0.05$, **$p<0.01$, ***$p<0.001$, ns not significant.
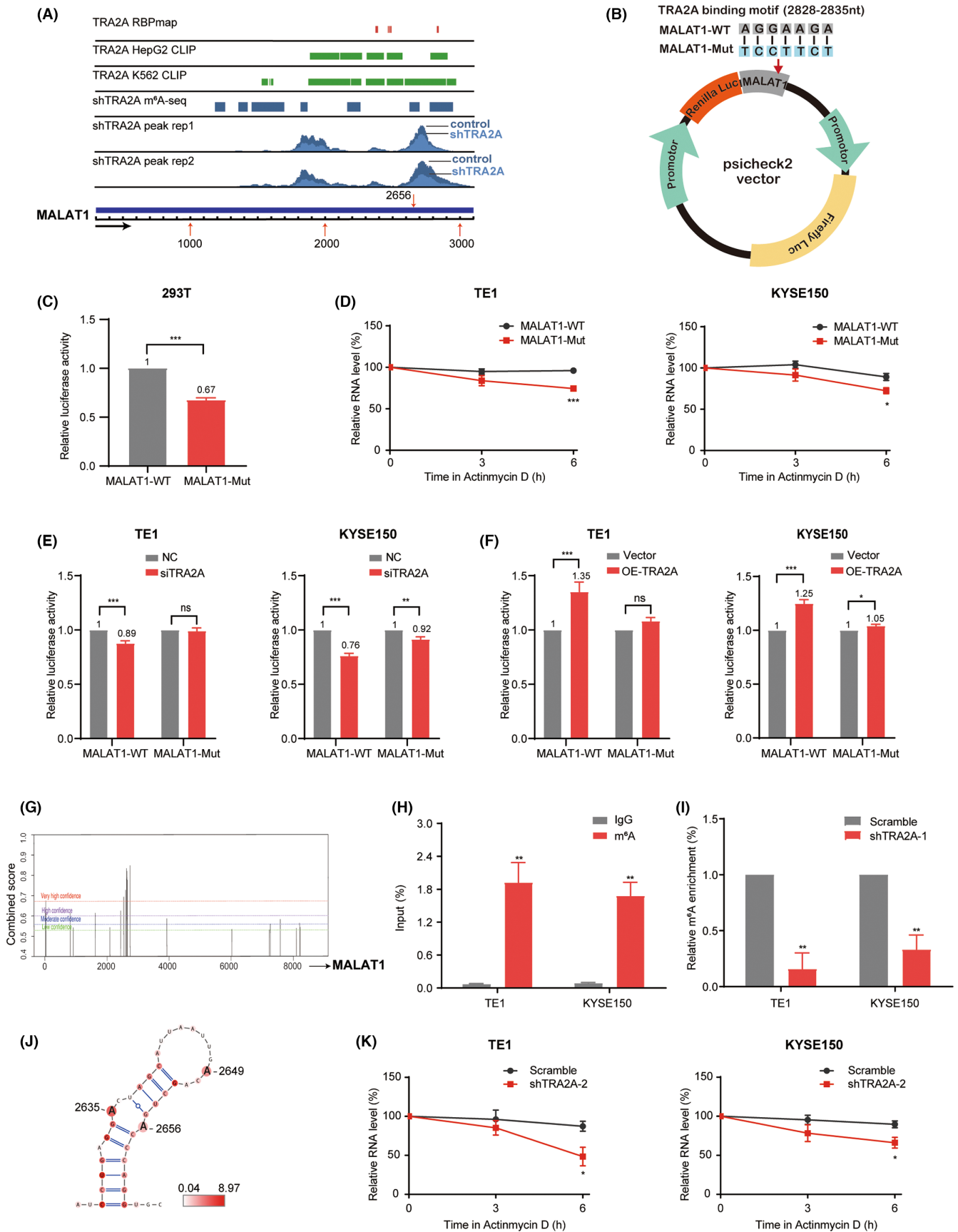
decrease (Figure 3I). We used the RNA2DMut tool to predict all possible single-point mutations and assess the impact on the predicted 2D structural ensemble diversity (ED) of lncRNA MALAT1.[22] Our results indicated that the mutated "A"s in the m^6A sites at 2635 - 2656nt would increase the ED value (Figure 3J), resulting in alternative folding or an unstable structure for MALAT1 mRNA. In support of this, RNA stability assays showed that ablation of TRA2A shortened the half-life of MALAT1 mRNA in both TE1 and KYSE150 cells (Figure 3K). Collectively, our findings suggested that knockdown of TRA2A impairs MALAT1 RNA stability by decreasing MALAT1 m^6A modification.

3.4 | TRA2A affects the m^6A-associated RBPs RBMX/KIAA1429

Given that MALAT1 expression and its m^6A methylation are simultaneously decreased following TRA2A ablation, we speculated that some m^6A methylation-associated RBPs might interact with TRA2A and mediate the regulation of MALAT1. By analyzing the expression correlation between TRA2A and classical m^6A proteins, including nine "writers" (METTL14, WTAP, RBM15, KIAA1429, ZC3H13, RBM15B, ZCCHC4, CBLL1, METTL16), three "erasers" (FTO, ALKBH5, ALKBH3) and eleven "readers" (YTHDF1-3, YTHDC1-2, IGF2BP1–3, HNRNPA2B1, RBMX, HNRNPC), we identified a set of proteins, including RBMX (Pearson correlation coefficient = 0.35) and KIAA1429 (Pearson correlation coefficient = 0.28), correlated with the expression of TRA2A in the esophageal cancer patients cohort in TCGA (Figures 4A and S1). Later, we verified that knockdown of TRA2A resulted in significant decreases at both the protein and mRNA levels of RBMX and KIAA1429 (Figure 4B,C). Moreover, the expression of MALAT1 was confirmed to be reduced or increased after silencing or overexpressing RBMX and KIAA1429 (Figure 4D–F). To explore the physical interaction between TRA2A and RBMX/KIAA1429, we transfected RBMX-Flag or KIAA1429-Flag plasmids into esophageal cells. Co-IP experiments showed an interaction between TRA2A and RBMX (Figure 4G), but not between TRA2A and KIAA1429.

3.5 | RBMX/KIAA1429 reverses the effects induced by the knockdown of TRA2A

We further investigated the functional roles of the RBMX/KIAA1429/MALAT1 pathway in TRA2A regulation. CCK-8 and colony formation assays demonstrated that knockdown of TRA2A reduced the proliferation of TE1 and KYSE150 cells in vitro, while ectopic expression of RBMX or KIAA1429 rescued the cell viability and growth (Figure 5A,B). In addition, we found that the expression of MALAT1 was rescued by both RBMX and KIAA1429 following TRA2A reduction (Figure 5C). These results suggested that TRA2A impairs MALAT1 in an RBMX/KIAA1429-dependent manner. Moreover, we

have previously found that knockdown of TRA2A inactivates the EZH2/β-catenin pathway,[9] so we postulated that enforced RBMX or KIAA1429 may rescue this inactivation. Indeed, western blot results showed that after TRA2A was inhibited in KYSE150 cells, EZH2/β-catenin protein levels were significantly reduced, but were restored after RBMX or KIAA1429 were overexpressed (Figure 5D).

3.6 | MALAT1, RBMX and KIAA1429 are clinically relevant to ESCA

To explore the genomic and transcriptomic characteristics of MALAT1, RBMX, and KIAA1429, we evaluated these based on esophageal cancer patients listed in the cBioPortal database (http://www.cbioportal.org/). We also examined the somatic mutations, copy number variations and expression profiles in esophageal cancer cell lines from CCLE (https://sites.broadinstitute.org/ccle/). As shown in Figure S2, genetic amplification and gene overexpression are the main alterations and account for ~7%, ~14%, and ~24% of patients for MALAT1, RBMX, and KIAA1429, respectively. Compared with the normal population, these three genes were also markedly induced in TCGA cohort and in esophageal cancer cell lines (Figure 6A and Table S5). Kaplan–Meier survival analysis demonstrated that patients with high MALAT1, RBMX, and KIAA1429 expression had shorter overall survival times (log-rank test, p = 4.30e-02, 4.00e-02, and 6.90e-02, respectively) than patients with low MALAT1, RBMX, and KIAA1429 (http://gepia.cancer-pku.cn/; Figure 6B). Together, the above results suggested that MALAT1, RBMX, and KIAA1429 are upregulated and clinically relevant to esophageal cancer.

3.7 | Nebivolol inhibits cell proliferation via targeting TRA2A

In colorectal cancer, indacaterol was identified as the inhibitor of SRSF6, another member of the SR family.[23] As TRA2A could promote cell proliferation and tumor progression, we wondered whether it could be considered a therapeutic target in ESCA. Distinct from the canonical SR factors, which contain two RRMs and one RS domain, both TRA2A and its paralog, TRA2B have only one RRM and two RS domains. Thus, we first compared the RRMs among TRA2 proteins, SRSF1 and SRSF6. We included SRSF1 because it is the founding member of the SR family. As shown in the percentage matrix (Figure S3A), the RRM of TRA2 proteins is more like RRM1, but not RRM2. Previous reports have indicated that deletion of RRM1 significantly affected target RNA recognition and alternative splicing.[23,24] As no crystal structure of TRA2A has been reported to date, we utilized a prediction model using alphafold2.[25] Based on the shape of indacaterol, we virtually screened the FDA-approved drugs to discover specific pharmacological inhibitors. Three compounds were selected for experimental evaluation (Table S6). We found that nebivolol, known as a potent antagonist of β1-adrenergic receptors and a weak antagonist
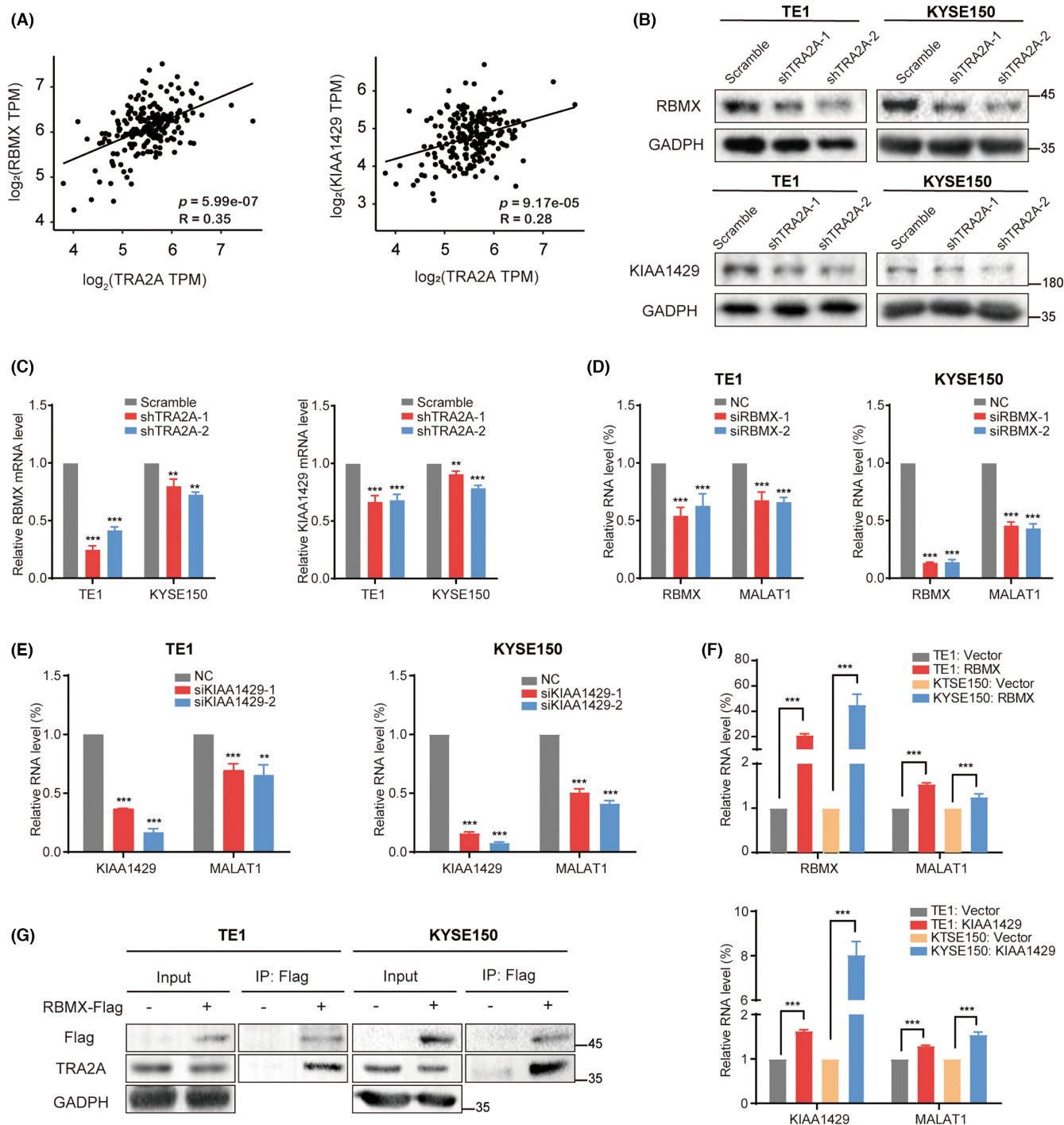
FIGURE 4 TRA2A interacts with m^{6}A methylation-associated RBPs. (A) Correlation between TRA2A and m^{6}A-associated RBPs in ESCA, $n = 197$. (B, C) Protein and mRNA levels of RBMX and KIAA1429 after TRA2A knockdown in TE1 and KYSE150 cells, $n = 3$. (D, E) RT-PCR showing the relative MALAT1 mRNA levels after silencing RBMX or KIAA1429, $n = 3$. (F) RT-PCR showing the relative MALAT1 mRNA levels after overexpressing RBMX or KIAA1429, $n = 3$. (G) Western blots showing the interaction between TRA2A and RBMX. Data are expressed as mean $\pm$ SEM; **$p < 0.01$, ***$p < 0.001$.

of β_2-adrenergic receptors,[26,27] could bind with TRA2A with a Vina score of −4.2 kcal/mol. From the binding pose and interactions with TRA2A, nebivolol resides in the hydrophobic pocket surrounded by several residues, such as Asp193, indicating that it binds to TRA2A stably (Figure 6C). Multiple alignment showed that Asp193 is conserved in the RRM1 domain, which corresponds

to the Asn87 position in SRSF1 (Figure S3B). A previous report found that the binding of RRM1 to target RNA drastically reduced when this residue was mutated.[24] Thus, we speculated that nebivolol may compete with the target RNA of TRA2A.

To further investigate this hypothesis and evaluate the antitumor effect, we tested nebivolol hydrochloride on KYSE150 cells.

FIGURE 5 TRA2A knockdown-mediated inhibition of cell proliferation is restored by RBMX/KIAA1429 overexpression. (A, B) CCK-8 and colony formation assays showing cell proliferation after transfection of siTRA2A or co-transfection of siTRA2A with RBMX or with KIAA1429, $n = 3$–5. (C) RT-PCR showing MALAT1 after transfection of siTRA2A or co-transfection of siTRA2A with RBMX or with KIAA1429, $n = 3$–4. (D) Western blots showing EZH2 and beta-catenin in KYSE150 cells. Data are expressed as mean ± SEM; *$p < 0.05$, **$p < 0.01$, ***$p < 0.001$.
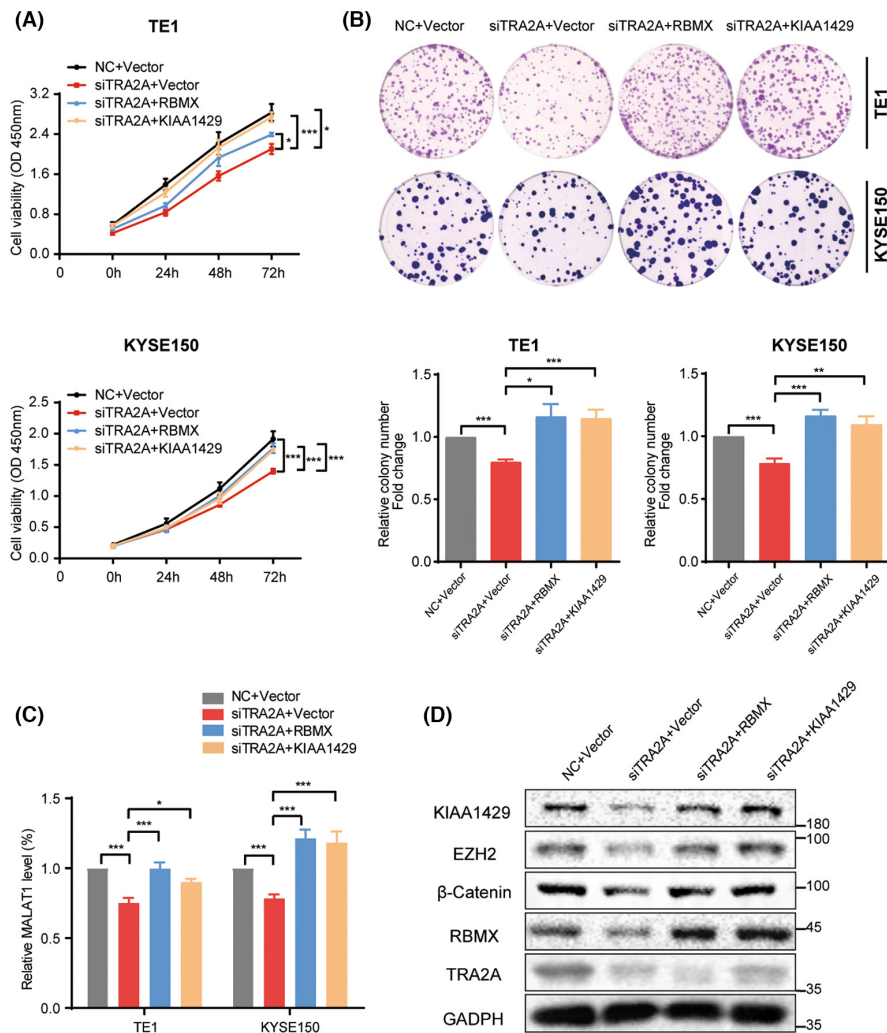
We found that nebivolol hydrochloride could kill KYSE150 cells in a dose-dependent manner and the IC_{50} concentration was at 12.02 μM (Figure 6D). Moreover, the inhibition rate increased with extended treatment time (Figure 6E) and nebivolol hydrochloride thoroughly inhibited cell colony formation at 10 μM (Figure 6F). As we speculated, MALAT1, RBMX, and KIAA1429 were decreased after nebivolol hydrochloride treatment, similarly to TRA2A silencing (Figure 6G). Cellular thermal shift assay showed that TRA2A was more stable above 49°C after treating with 50 μM nebivolol hydrochloride for 3h (Figure 6H). In addition, RIP results indicated that the bound MALAT1 was decreased by pulling down with TRA2A antibody after treating with nebivolol hydrochloride (Figure 6I). These results suggested that nebivolol directly binds to TRA2A to compete with TRA2A–MALAT1 binding in vitro. Furthermore, the half-life of MALAT1 mRNA was shortened after nebivolol hydrochloride treatment (Figure 6J). Also, we found that $\beta_{1/2}$-adrenergic receptors were expressed at a low level in all CCLE esophageal cancer cell lines (Table S7), indicating that $\beta_{1/2}$-adrenergic receptors are not the major target of nebivolol in resulting the growth inhibition in ESCA. Together, the above results suggested that nebivolol could be a potent inhibitor to interfere with TRA2A–MALAT1 signaling in esophageal cancer.

4 | DISCUSSION

N^6-methyladenosine is one of the most common chemical modifications in eukaryotic messenger RNAs and non-coding RNAs.[28,29] Three major types of regulator, namely writers, erasers, and readers, participate in this reversible epigenetic modification. The m^6A methyltransferase complex, including METTL3, METTL14, WTAP, and their cofactors KIAA1429 and RBM15, catalyzes m^6A modification as the writer.[30] The α-ketoglutarate (αKG)-dependent and Fe (II)-dependent demethylases, such as FTO and ALKBH5, can remove the m^6A marks from RNA, serving as the erasers.[31,32] The YT521-B homology (YTH) domain family, insulin-like growth factor 2 mRNA binding proteins (IGF2BPs), and heterogeneous nuclear ribonucleoproteins (hnRNPs) recognize m^6A sites and process different target RNAs as the readers.[33] The functional roles of these m^6A-associated proteins have been elucidated in development and various diseases.[28,34]

Inspired by the report that TRA2A directly interacts with METTL3 in HepG2 cells,[21] we investigated its role in m^6A methylation. We found that TRA2A affects the lncRNA global m^6A level in esophageal cancer. We confirmed the interaction between TRA2A and METTL3, and found that TRA2A affected the reader RBMX (hnRNPG) and
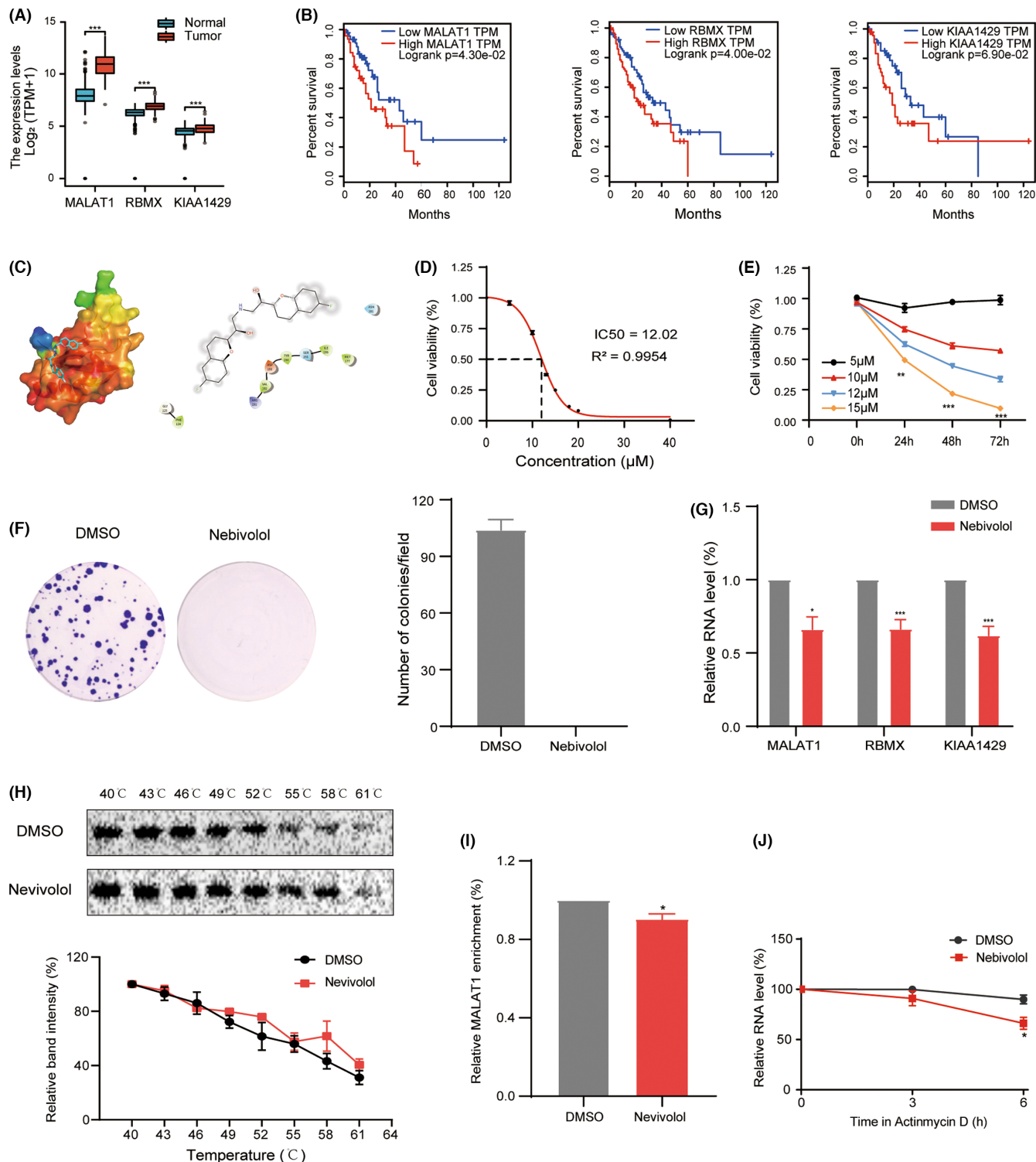
FIGURE 6 Clinical relevance of the TRA2A–MALAT1–methylation axis. (A) Expression levels of MALAT1, RBMX, and KIAA1429 in ESCA cohorts ($n = 848$). (B) Overall survival of esophageal cancer patients from the GEPIA database, with comparison between the low and high MALAT1/RBMX/KIAA1429 expression groups, $n = 182$. (C) Binding mode of nebivolol hydrochloride with TRA2A from molecular docking. (D) IC_{50} fitting curve for nebivolol hydrochloride on KYSE150 cells. (E) KYSE150 cells were treated with different concentration of nebivolol hydrochloride and incubated for 0–72h, statistical significance was assessed using one-way analysis of variance, $n = 4$. (F) Colony formation assays showing cell proliferation after cells were treated with nebivolol hydrochloride at 10 μM, $n = 3$. (G) RT-PCR showing MALAT1, RBMX, and KIAA1429 after cells were treated with nebivolol hydrochloride at 12 μM for 48h, $n = 3$. (H) Western blots and the quantification showing the TRA2A level after treatment with 50 μM nebivolol hydrochloride for 3h in KYSE150 cells. (I) RIP assay showing the MALAT1 level after treatment with nebivolol hydrochloride at 50 μM for 4.5h in KYSE150 cells, $n = 3$. (J) MALAT1 decay rate was determined in KYSE150 cells after treatment with 12 μM nebivolol hydrochloride for 48h, $n = 3$. Data are expressed as mean ± SEM; $**p < 0.01$, $***p < 0.001$.

FIGURE 7 Illustration summarizes the findings of TRA2A-mediated m⁶A regulation.
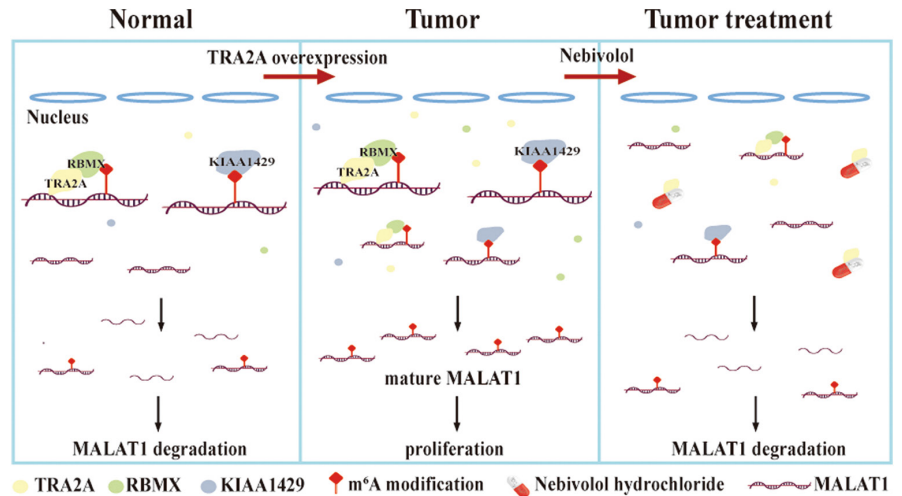
the writer KIAA1429 to regulate MALAT1 methylation and stability. RBMX interacts with m^6A-modified nascent pre-mRNA to modulate splicing and maintain the chromatin state in myeloid leukemia.[35,36] Accumulating research has shown that both KIAA1429 and RBMX contribute to tumor progression.[37–40] However, the detailed mechanism of TRA2A regulates METTL3, RBMX, and KIAA1419 is not completely known and should be further investigated.

Accumulating studies have demonstrated that MALAT1 is enriched with methylation marks.[41–44] These dynamic modifications regulate the scaffolding for RBPs as well as miRNAs, by altering MALAT1 structure and stability. MALAT1 has also been linked with the development and metastasis of a variety of cancers.[45,46] In esophageal squamous cell carcinoma, MALAT1 is upregulated and promotes proliferation and tumor growth.[9,47] Here, we proposed that TRA2A coordinates with multiple methylation proteins to regulate MALAT1 and malignant transformation. Moreover, we also provided evidence that nebivolol inhibits cell proliferation by interfering with TRA2A-MALAT1 signaling (Figure 7). As SR proteins may harbor a similar RRM domain, it is possible that another SR is also the target of nebivolol. Thus, further studies are warranted to exploit TRA2A as a novel therapeutic target for esophageal cancer therapy.

Genomic and transcriptome studies have revealed that AS is a fundamental mechanism in carcinogenesis and drug resistance.[48,49] Previously, we and others have investigated the AS pattern in ESCA cells and patient tissues using Pacbio long-read sequencing or short-read RNA-seq platforms.[10,50,51] These analyses suggested that aberrant splicing disturbs key signaling pathways and is associated with clinical outcomes. In the current study, we demonstrated that splicing factor TRA2A also regulates the m^6A modifications on lncRNAs. Indeed, high-throughput sequencing of RNAs isolated with SR proteins revealed that they usually bind multiple ncRNAs. For example, HITS-CLIP analysis revealed that SRSF1 binds a diverse pool of RNA transcripts, including mRNAs, miRNAs, snoRNAs, and long intergenic transcripts.[52] Thus, we speculated that other SR proteins might modify ncRNAs in a similar manner. Distinct from their canonical function in mRNA splicing, SR proteins largely expand their regulatory function by interfering with ncRNA processing and modification. As a prototype, our results on the modulating of MALAT1 by TRA2A highlighted the essential role of SR protein–ncRNA interactions in lncRNA m^6A modification and ESCA progression.

AUTHOR CONTRIBUTIONS

JX designed and supervised the research. MB conducted the main experiments. SH conducted the main bioinformatics analysis. KL, QC, YC, XZ, LJ, LL, and GD contributed to technical support. MB and JX wrote the manuscript. All authors read and approved the final manuscript.

CONFLICT OF INTERESTS

The authors declare no conflict of interest.

ETHICS STATEMENT

Approval of the research protocol by an Institutional Review Board: N/A.

Informed Consent: N/A.

Registry and the Registration No. of the study/trial: N/A.

Animal Studies: All animal care and experimental protocols were approved by the Committee of Guangdong Medical University.

ORCID

Jianzhen Xu 🆔 https://orcid.org/0000-0002-0697-9075

REFERENCES

1. Sung H, Ferlay J, Siegel RL, et al. Global cancer statistics 2020: GLOBOCAN estimates of incidence and mortality worldwide for 36 cancers in 185 countries. *CA Cancer J Clin*. 2021;71:209-249.

2. Kelly RJ. Emerging multimodality approaches to treat localized esophageal cancer. *J Natl Compr Canc Netw*. 2019;17:1009-1014.

3. Hategan M, Cook N, Prewett S, Hindmarsh A, Qian W, Gilligan D. Trimodality therapy and definitive chemoradiotherapy for esophageal cancer: a single-center experience and review of the literature. *Dis Esophagus*. 2015;28:612-618.

4. Olsen CM, Pandeya N, Green AC, Webb PM, Whiteman DC, Australian Cancer Study. Population attributable fractions of adenocarcinoma of the esophagus and gastroesophageal junction. *Am J Epidemiol*. 2011;174:582-590.

5. Thrift AP. Global burden and epidemiology of Barrett oesophagus and oesophageal cancer. *Nat Rev Gastroenterol Hepatol*. 2021;18:432-443.

6. Mao C, Zeng X, Zhang C, et al. Mechanisms of pharmaceutical therapy and drug resistance in esophageal cancer. *Front Cell Dev Biol*. 2021;9:612451.

7. Wu H, Chen S, Yu J, et al. Single-cell transcriptome analyses reveal molecular signals to intrinsic and acquired paclitaxel resistance in esophageal squamous cancer cells. *Cancer Lett*. 2018;420:156-167.

8. Long JC, Caceres JF. The SR protein family of splicing factors: master regulators of gene expression. *Biochem J*. 2009;417:15-27.

9. Zhao X, Chen Q, Cai Y, et al. TRA2A binds with LncRNA MALAT1 to promote esophageal cancer progression by regulating EZH2/beta-catenin pathway. *J Cancer*. 2021;12:4883-4890.

10. Ding J, Li C, Cheng Y, et al. Alterations of RNA splicing patterns in esophagus squamous cell carcinoma. *Cell Biosci*. 2021;11:36.

11. Kuwabara PE, Kimble J. A predicted membrane protein, TRA-2A, directs hermaphrodite development in *Caenorhabditis elegans*. *Development*. 1995;121(9):2995-3004.

12. Tan Y, Hu X, Deng Y, Yuan P, Xie Y, Wang J. TRA2A promotes proliferation, migration, invasion and epithelial mesenchymal transition of glioma cells. *Brain Res Bull*. 2018;143:138-144.

13. Liu T, Sun H, Zhu D, et al. TRA2A promoted paclitaxel resistance and tumor progression in triple-negative breast cancers via regulating alternative splicing. *Mol Cancer Ther*. 2017;16:1377-1388.

14. Li L, Miao H, Chang Y, et al. Multidimensional crosstalk between RNA-binding proteins and noncoding RNAs in cancer biology. *Semin Cancer Biol*. 2021;75:84-96.

15. Jonas K, Calin GA, Pichler M. RNA-binding proteins as important regulators of Long non-coding RNAs in cancer. *Int J Mol Sci*. 2020;21:2969.

16. Yu G, Wang LG, He QY. ChIPseeker: an R/Bioconductor package for ChIP peak annotation, comparison and visualization. *Bioinformatics*. 2015;31:2382-2383.

17. Bao Z, Yang Z, Huang Z, Zhou Y, Cui Q, Dong D. LncRNADisease 2.0: an updated database of long non-coding RNA-associated diseases. *Nucleic Acids Res*. 2019;47:D1034-D1037.

18. Gong J, Cai C, Liu X, et al. ChemMapper: a versatile web server for exploring pharmacology and chemical structure association based on molecular 3D similarity method. *Bioinformatics*. 2013;29:1827-1829.

19. Eberhardt J, Santos-Martins D, Tillack AF, Forli S. AutoDock Vina 1.2.0: new docking methods, expanded force field, and python bindings. *J Chem Inf Model*. 2021;61:3891-3898.

20. Lin L, Lin K, Wu X, et al. Potential inhibitors of Fascin from a database of marine natural products: a virtual screening and molecular dynamics study. *Front Chem*. 2021;9:719949.

21. An S, Huang W, Huang X, et al. Integrative network analysis identifies cell-specific trans regulators of m6A. *Nucleic Acids Res*. 2020;48:1715-1729.

22. Moss WN. RNA2DMut: a web tool for the design and analysis of RNA structure mutations. *RNA*. 2018;24:273-286.

23. Wan L, Yu W, Shen E, et al. SRSF6-regulated alternative splicing that promotes tumour progression offers a therapy target for colorectal cancer. *Gut*. 2019;68:118-129.

24. Clery A, Krepl M, Nguyen CKX, et al. Structure of SRSF1 RRM1 bound to RNA reveals an unexpected bimodal mode of interaction and explains its involvement in SMN1 exon7 splicing. *Nat Commun*. 2021;12:428.

25. Varadi M, Anyango S, Deshpande M, et al. AlphaFold protein structure database: massively expanding the structural coverage of protein-sequence space with high-accuracy models. *Nucleic Acids Res*. 2022;50:D439-D444.

26. Van de Water A, Janssens W, Van Neuten J, et al. Pharmacological and hemodynamic profile of nebivolol, a chemically novel, potent, and selective beta 1-adrenergic antagonist. *J Cardiovasc Pharmacol*. 1988;11:552-563.

27. Pauwels PJ, Leysen JE, Janssen PA. Beta-adrenoceptor-mediated cAMP accumulation in cardiac cells: effects of nebivolol. *Eur J Pharmacol*. 1989;172:471-479.

28. Fu Y, Dominissini D, Rechavi G, He C. Gene expression regulation mediated through reversible m(6)a RNA methylation. *Nat Rev Genet*. 2014;15:293-306.

29. Ma S, Chen C, Ji X, et al. The interplay between m6A RNA methylation and noncoding RNA in cancer. *J Hematol Oncol*. 2019;12:121.

30. Huang H, Weng H, Chen J. M(6)a modification in coding and non-coding RNAs: roles and therapeutic implications in cancer. *Cancer Cell*. 2020;37:270-288.

31. Jia G, Fu Y, Zhao X, et al. N6-methyladenosine in nuclear RNA is a major substrate of the obesity-associated FTO. *Nat Chem Biol*. 2011;7:885-887.

32. Zheng G, Dahl JA, Niu Y, et al. ALKBH5 is a mammalian RNA demethylase that impacts RNA metabolism and mouse fertility. *Mol Cell*. 2013;49:18-29.

33. He L, Li H, Wu A, Peng Y, Shu G, Yin G. Functions of N6-methyladenosine and its role in cancer. *Mol Cancer*. 2019;18:176.

34. Roundtree IA, Evans ME, Pan T, He C. Dynamic RNA modifications in gene expression regulation. *Cell*. 2017;169:1187-1200.

35. Zhou KI, Shi H, Lyu R, et al. Regulation of Co-transcriptional pre-mRNA splicing by m(6)a through the low-complexity protein hnRNPG. *Mol Cell*. 2019;76:70-81.e9.

36. Prieto C, Nguyen DTT, Liu Z, et al. Transcriptional control of CBX5 by the RNA binding proteins RBMX and RBMXL1 maintains chromatin state in myeloid leukemia. *Nat Cancer*. 2021;2:741-757.

37. Zhang X, Dai XY, Qian JY, et al. SMC1A regulated by KIAA1429 in m6A-independent manner promotes EMT progress in breast cancer. *Mol Ther Nucleic Acids*. 2022;27:133-146.

38. Lan T, Li H, Zhang D, et al. KIAA1429 contributes to liver cancer progression through N6-methyladenosine-dependent post-transcriptional modification of GATA3. *Mol Cancer*. 2019;18:186.

39. Tang J, Han T, Tong W, Zhao J, Wang W. N(6)-methyladenosine (m(6)a) methyltransferase KIAA1429 accelerates the gefitinib resistance of non-small-cell lung cancer. *Cell Death Discov*. 2021;7:108.

40. Zhang Z, Zhang C, Yang Z, et al. M(6)a regulators as predictive biomarkers for chemotherapy benefit and potential therapeutic targets for overcoming chemotherapy resistance in small-cell lung cancer. *J Hematol Oncol*. 2021;14:190.

41. Chang YZ, Chai RC, Pang B, et al. METTL3 enhances the stability of MALAT1 with the assistance of HuR via m6A modification and activates NF-kappaB to promote the malignant progression of IDH-wildtype glioma. *Cancer Lett*. 2021;511:36-46.

42. Jin D, Guo J, Wu Y, et al. M(6)a mRNA methylation initiated by METTL3 directly promotes YAP translation and increases YAP activity by regulating the MALAT1-miR-1914-3p-YAP axis to induce NSCLC drug resistance and metastasis. *J Hematol Oncol*. 2019;12:135.

43. Liu N, Zhou KI, Parisien M, Dai Q, Diatchenko L, Pan T. N6-methyladenosine alters RNA structure to regulate binding of a low-complexity protein. *Nucleic Acids Res*. 2017;45:6051-6063.

44. Wang X, Liu C, Zhang S, et al. N(6)-methyladenosine modification of MALAT1 promotes metastasis via reshaping nuclear speckles. *Dev Cell.* 2021;56:702-715.e8.

45. Shen WJ, Zhang F, Zhao X, Xu J. LncRNAs and esophageal squamous cell carcinoma – implications for pathogenesis and drug development. *J Cancer.* 2016;7:1258-1264.

46. Liu SJ, Dang HX, Lim DA, Feng FY, Maher CA. Long noncoding RNAs in cancer metastasis. *Nat Rev Cancer.* 2021;21:446-460.

47. Hu L, Wu Y, Tan D, et al. Up-regulation of long noncoding RNA MALAT1 contributes to proliferation and metastasis in esophageal squamous cell carcinoma. *J Exp Clin Cancer Res.* 2015;34:7.

48. Siegfried Z, Karni R. The role of alternative splicing in cancer drug resistance. *Curr Opin Genet Dev.* 2018;48:16-21.

49. Dvinge H, Kim E, Abdel-Wahab O, Bradley RK. RNA splicing factors as oncoproteins and tumour suppressors. *Nat Rev Cancer.* 2016;16:413-430.

50. Cheng YW, Chen YM, Zhao QQ, et al. Long read single-molecule real-time sequencing elucidates transcriptome-wide heterogeneity and complexity in esophageal squamous cells. *Front Genet.* 2019;10:915.

51. Mao S, Li Y, Lu Z, et al. Survival-associated alternative splicing signatures in esophageal carcinoma. *Carcinogenesis.* 2019;40:121-130.

52. Lu Z, Guo JK, Wei Y, et al. Structural modularity of the XIST ribonucleoprotein complex. *Nat Commun.* 2020;11:6163.

SUPPORTING INFORMATION

Additional supporting information can be found online in the Supporting Information section at the end of this article.